Available online at www.sciencedirect.com
SCIENCE DIRECT®
Journal of Sound and Vibration 277 (2004) 49–71
JOURNAL OF SOUND AND VIBRATION
www.elsevier.com/locate/jsvi

A new approach for free vibration analysis of arches with effects of shear deformation and rotary inertia considered

Jong-Shyong Wu*, Lieh-Kwang Chiang

Department of Naval Architecture and Marine Engineering, National Cheng-Kung University, Tainan 701, Taiwan, ROC

Received 26 February 2003; accepted 20 August 2003

Abstract

When the effects of both the shear deformation and rotary inertia are considered, the literature regarding the free vibration analysis of circular arches using the finite arch elements is rare. To the authors' knowledge, Int. J. Numer. Methods Eng. 52 (2001) 273–286 is the latest work of the literature that deals with this in detail. Since the procedures for deriving the stiffness and mass matrices of the arch element are tedious and complicated in available literature, this paper tries to present a simple approach to overcome these drawbacks. First, the three functions for the radial (or normal), tangential and rotational displacements of an arch element are assumed. Since each function consists of six integration constants, one has 18 unknown constants for the three displacement functions. Next, from the last three displacement functions, the three force–displacement differential equations and the three static equilibrium equations for the arch element, one obtains three polynomial expressions. Equating to zero the coefficients of the terms in each of the last three expressions, respectively, one obtains 18 equations as functions of the 18 unknown constants. Excluding the 6 dependent ones among the last 18 equations, one obtains 12 independent equations. Solving for the last 12 independent equations yielded a unique solution in terms of six unknown constants. Finally, imposing the boundary conditions at the two ends of an arch element determines the last six unknown constants and completely defines the three displacement functions. By means of the displacement functions, one may calculate the stiffness and mass matrices of each arch element and then perform the free vibration analysis of the arches. Good agreement between the results of this paper and those of the existing literature validated the presented approach.

1. Introduction

While the application of finite elements to flat structures such as beams and plates is well established, the solution for the curved structures, such as arches, rings and shells, is not yet

*Corresponding author. Tel.: +886-6-258-7376; fax: +886-6-280-8458.
E-mail address: jswu@mail.ncku.edu.tw (J.-S. Wu).

0022-460X/$ - see front matter
doi:10.1016/j.jsv.2003.08.012

completely understood [1]. Thus, many researchers devoted themselves to this field. Since the in-plane and out-of-plane behaviors of the curved beams are usually tackled separately, only the information regarding (in-plane) vibrations of arches is reviewed here. Most of the existing reports aim at derivations of displacement functions (or shape functions) and stiffness matrices of the arch (curved beam) elements [2–8]. Although these reports are very useful for the static analysis of the arches, the mass matrix of the arch element is also required for the dynamic analysis of arches. However, information on this aspect is rare and Refs. [1,9–13] are the few papers most concerned.

Neglecting the effect of rotary inertia (RI) and using the two functions for the radial and tangential displacements, the stiffness matrix and consistent mass matrix of the arch element were derived in "explicit" forms by Sabir and Ashwell [1] and Petyt and Fleischer [9]. In Ref. [10], by considering the effects of RI and warping torsion and neglecting the effect of shear deformation (SD), both the stiffness and mass matrices of the thin-walled (spatial) curved beam element were derived from the energy variation theory. In Ref. [11], the explicit shape functions of Ref. [8] were used to derive the stiffness matrix and consistent mass matrix of the arch element by using the energy variation theory and the unit-displacement method, respectively. In Ref. [14], by considering the effect of RI and neglecting that of SD, the stiffness matrix and consistent mass matrix of the arch element were derived in "implicit" forms based on the three functions given by Ref. [3] for the radial displacement, tangential displacement and the rotational angle. The element stiffness matrix was obtained from the force–displacement relations given by Ref. [3] and the element mass matrix was directly derived from the equation of kinetic energy for the arch element. Comparing with the 18 explicit shape functions reported in Ref. [8] and the 100 unknown constants for the shape functions of Ref. [13], shape functions given by Ref. [14] are in implicit matrix form and have advantages of easy derivation, easy computer programming and mistakes easy to get rid of.

Although the formulation of Ref. [14] is much simpler than that of Ref. [8], the effect of SD was neglected by the former and was considered by the latter. Besides, the displacement functions for the arch element in Ref. [14] were obtained from Ref. [3], where the procedures for deriving the displacement functions were complicated. To improve all the above-mentioned defects of Refs. [14,3], this paper presents a simple, straightforward and systematic technique to derive the displacement functions for the radial (or normal), tangential and rotational displacements of an arch element by taking account of the effects of both the SD and RI. First, the three functions for the radial (or normal), tangential and rotational displacements of an arch element are assumed. Next, the last three displacement functions were substituted into the three force–displacement relations to determine the three element forces. Finally, the last three element forces were further substituted into the three static equilibrium equations for the infinitesimal arch element to yield three polynomial expressions. By respectively equating to zero the constant term and the coefficients of the terms θ, $\sin\theta$, $\cos\theta$, $\theta\sin\theta$ and $\theta\cos\theta$, in each of the last three expressions, where θ is the angular co-ordinate for the arch element, one obtains the 18 equations as functions of the 18 unknown integration constants. Solving the last 18 equations and incorporating the six nodal displacements at the two ends of the arch element, one may determine all the integration constants and completely define the three displacement functions. Since the force–displacement relationships for the Timoshenko arch element (with SD considered) are different from those for the Euler arch element (with SD neglected), the procedures for deriving the displacement functions of the Timoshenko arch element must be repeated for deriving those of the Euler arch element and then

the results are combined to give the three displacement functions available for both the Timoshenko arch element and the Euler arch element. This was also true for deriving the stiffness matrix available for the Timoshenko and Euler arch elements.

Once the displacement functions for an arch element were defined, the approach of Ref. [14] is used to perform the free vibration analysis of various circular arches. In addition to the complicated consistent-mass model, the simple lumped-mass model was also tried and good agreement between the results obtained from the two models was achieved. For convenience, an arch neglecting the effects of both the SD and the RI was called the "Euler arch", an arch considering only the effect of RI was called the "rotary arch" and an arch considering effects of both SD and RI was called the "Timoshenko arch". The influence of thickness ratio (a/R) and supporting conditions on the natural frequencies and mode shapes of the Euler arch, the rotary arch and the Timoshenko arch were studied, where a is the radial thickness and R is the average radius of the circular arch.

2. Displacement functions

For the arch element shown in Fig. 1, if the x-axis is the symmetric axis for the cross-section of the arch, then the functions for the radial displacement u_x, the circumferential displacement u_θ and the rotational angle ψ_y are to take the forms [3,8]

$$u_x = A_1 + A_2\theta + A_3 \sin\theta + A_4 \cos\theta + A_5\theta \sin\theta + A_6\theta \cos\theta, \tag{1a}$$

$$u_\theta = B_1 + B_2\theta + B_3 \sin\theta + B_4 \cos\theta + B_5\theta \sin\theta + B_6\theta \cos\theta, \tag{1b}$$

$$\psi_y = \frac{1}{R}(C_1 + C_2\theta + C_3 \sin\theta + C_4 \cos\theta + C_5\theta \sin\theta + C_6\theta \cos\theta), \tag{1c}$$

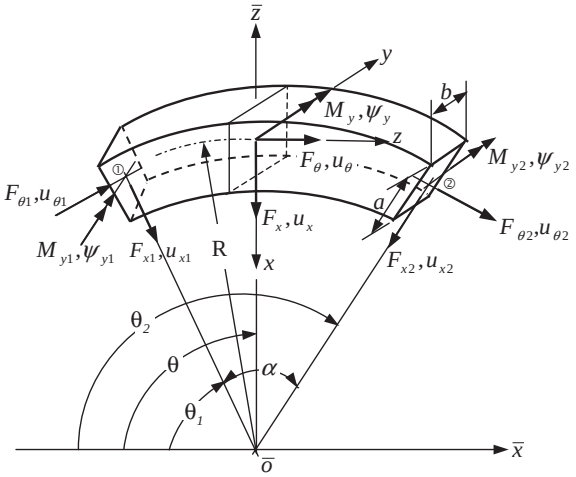

Fig. 1. Definitions of the element displacements (u_x, u_θ, ψ_y) and the corresponding element forces (F_x, F_θ, M_y) for an in-plane curved beam (arch) element and the associated reference local and global co-ordinate systems, xyz and $\bar{x}\,\bar{y}\,\bar{z}$.

where A_1–A_6, B_1–B_6 and C_1–C_6 are the integration constants determined by the boundary conditions of the arch element.

If the effect of SD is considered, then the relationships between the element forces (F_x, F_θ, M_y) and the element displacements (u_x, u_θ, ψ_y) are given by [8,15]

$$F_x = \frac{k'AG}{R}(u'_x + u_\theta - R\psi_y), \tag{2a}$$

$$F_\theta = \frac{EA}{R}(u'_\theta - u_x), \tag{2b}$$

$$M_y = \frac{EI_y}{R^2}R\psi'_y, \tag{2c}$$

where F_x, F_θ and M_y are the shear force, tangential force and bending moment in the positive x, z and y directions, respectively, with xyz being the local reference co-ordinate system as shown in Fig. 1, G is the shear modulus, k' is the shear coefficient, A is the cross-sectional area, R is the average radius of curvature of the arch element and I_y is the moment of inertia of the area A about the y-axis given by [3]

$$I_y = \int_A \frac{x^2}{1-(x/R)}\,\mathrm{d}A. \tag{3}$$

In Eqs. (2a)–(2c), the primes denote differentiation with respect to the angular co-ordinate θ.

Static equilibrium of the infinitesimal curved beam element shown in Fig. 1 requires that [3,15]

$$M'_y + RF_x = 0, \tag{4a}$$

$$F'_x + F_\theta = 0, \tag{4b}$$

$$F'_\theta - F_x = 0. \tag{4c}$$

Substituting Eq. (1) into Eq. (2) and then introducing the resulting expressions into Eq. (4), one obtains three equations. Equating to zero the constant term and the coefficients of the terms θ, $\sin\theta$, $\cos\theta$, $\theta\sin\theta$ and $\theta\cos\theta$, respectively, in each of the last three equations, one obtains the following 18 equations for the integration constants A_1–A_6, B_1–B_6 and C_1–C_6:

$$A_2 - C_1 = -B_1, \tag{5a}$$

$$C_2 = B_2, \tag{5b}$$

$$A_4 - A_5 + (1+r_s)C_3 + 2r_sC_6 = B_3, \tag{5c}$$

$$A_3 + A_6 - (1+r_s)C_4 + 2r_sC_5 = -B_4, \tag{5d}$$

$$A_6 + (1+r_s)C_5 = B_5, \tag{5e}$$

$$A_5 - (1+r_s)C_6 = -B_6, \tag{5f}$$

$$r_e A_1 + C_2 = (1 + r_e)B_2, \tag{6a}$$

$$A_2 = 0, \tag{6b}$$

$$(1 + r_e)A_3 + 2A_6 - C_4 + C_5 = -(1 + r_e)B_4 + (1 + r_e)B_5, \tag{6c}$$

$$(1 + r_e)A_4 - 2A_5 + C_3 + C_6 = (1 + r_e)B_3 + (1 + r_e)B_6, \tag{6d}$$

$$(1 + r_e)A_5 - C_6 = -(1 + r_e)B_6, \tag{6e}$$

$$(1 + r_e)A_6 + C_5 = (1 + r_e)B_5, \tag{6f}$$

$$(1 + r_e)A_2 - C_1 = -B_1, \tag{7a}$$

$$C_2 = B_2, \tag{7b}$$

$$(1 + r_e)A_4 - (1 + r_e)A_5 + C_3 = (1 + r_e)B_3 + 2r_e B_6, \tag{7c}$$

$$(1 + r_e)A_3 + (1 + r_e)A_6 - C_4 = -(1 + r_e)B_4 + 2r_e B_5, \tag{7d}$$

$$(1 + r_e)A_6 + C_5 = (1 + r_e)B_5, \tag{7e}$$

$$(1 + r_e)A_5 - C_6 = -(1 + r_e)B_6, \tag{7f}$$

where

$$r_s = EI_y/(k'GA \cdot R^2), \tag{8}$$

$$r_e = EA/(k'GA). \tag{9}$$

In the last two equations, the subscripts of the symbols r_s and r_e denotes the "shear" deformation ratio and "extension" ratio, respectively.

It is noted that, in order to represent the values of A_i and C_i ($i = 1$–6) in terms of B_i ($i = 1, 2\ldots$), the foregoing 18 equations were rewritten from the forms $f_1(A_i, B_i, C_i) = 0$ to the ones $f_2(A_i, C_i) = f_3(B_i)$, where $f_j(X)$ denotes a function of X.

From Eqs. (5a), (5b), (6a) and (6b), one obtains

$$A_1 = B_2, \quad A_2 = 0, \quad C_1 = B_1, \quad C_2 = B_2 \tag{10}$$

and from Eqs. (5e), (5f), (6e) and (6f) one has

$$A_5 = -B_6, \quad A_6 = B_5, \quad C_5 = C_6 = 0. \tag{11}$$

When the relations given by Eqs. (10) and (11) are introduced into Eqs. (5)–(7), one obtains the following 12 independent equations for the 12 unknowns A_i and C_i ($i = 1$–6):

$$\begin{cases} C_1 = B_1, \\ C_2 = B_2, \\ A_4 + (1 + r_s)C_3 = B_3 - B_6, \\ A_3 - (1 + r_s)C_4 = -B_4 - B_5, \\ A_5 = -B_6, \\ A_6 = B_5, \end{cases}$$

$$\begin{cases} A_1 = B_2, \\ A_2 = 0, \\ (1 + r_e)A_3 + 2A_6 - C_4 = -(1 + r_e)B_4 + (1 + r_e)B_5, \\ (1 + r_e)A_4 - 2A_5 + C_3 = (1 + r_e)B_3 + (1 + r_e)B_6, \end{cases}$$

$$\begin{cases} (1 + r_e)A_4 + C_3 = (1 + r_e)B_3 - (1 - r_e)B_6, \\ (1 + r_e)A_3 - C_4 = -(1 + r_e)B_4 - (1 - r_e)B_5. \end{cases} \tag{12}$$

The solutions for the last 12 equations are

$$\begin{cases} A_1 = B_2, \\ A_2 = 0, \\ A_3 = -B_4 - S_2B_5, \\ A_4 = B_3 - S_2B_6, \\ A_5 = -B_6, \\ A_6 = B_5, \end{cases} \tag{13a}$$

$$\begin{cases} C_1 = B_1, \\ C_2 = B_2, \\ C_3 = -S_1B_6, \\ C_4 = S_1B_5, \\ C_5 = 0, \\ C_6 = 0, \end{cases} \tag{13b}$$

where

$$S_1 = 2r_e/(R_eR_s - 1), \tag{14}$$

$$S_2 = 1 - (1 + r_s)S_1, \tag{15}$$

$$R_e = 1 + r_e, \tag{16}$$

$$R_s = 1 + r_s. \tag{17}$$

For convenience of computer calculations, one sets

$$B_1 = G_5, \quad B_i = G_{i-1} \quad (i = 2-5), \quad B_6 = G_6. \tag{18}$$

Substituting Eq. (18) into Eq. (13) and then introducing the resulting values of A_i, B_i and C_i ($i = 1-6$) into Eqs. (1a)–(1c) one obtains

$$\begin{aligned} u_x = {} & G_1 + G_2 \cos\theta - G_3 \sin\theta + G_4(\theta \cos\theta - S_2 \sin\theta) \\ & + G_6(-\theta \sin\theta - S_2 \cos\theta), \end{aligned} \tag{19a}$$

$$u_\theta = G_1\theta + G_2 \sin\theta + G_3 \cos\theta + G_4\theta \sin\theta + G_5 + G_6\theta \cos\theta, \tag{19b}$$

$$\psi_y = \frac{1}{R}[G_1\theta + G_4(S_1 \cos\theta) + G_5 + G_6(-S_1 \sin\theta)]. \tag{19c}$$

If the effect of SD is neglected, then Eq. (2) reduces to [3,14]

$$F_x = F'_\theta, \tag{20a}$$

$$F_\theta = \frac{EA}{R}(u'_\theta - u_x) - \frac{M_y}{R}, \tag{20b}$$

$$M_y = \frac{EI_y}{R^2}(u''_x + u_x) \tag{20c}$$

but the static equilibrium equations given by Eq. (4) remain unchanged [3].

From Eqs. (4b) and (4c) one obtains

$$F''_\theta + F_\theta = 0 \tag{21}$$

and neglecting the SD yields the following relationship:

$$R\psi_y - (u'_x + u_\theta) = 0. \tag{22}$$

Following the same previous procedures for the case of considering the SD, i.e., substituting Eq. (1) into Eq. (20) and then introducing the resulting expressions into Eqs. (4a) and (21), together with the result of substituting Eq. (1) into Eq. (22), one obtains three equations. Equating to zero the constant term and the coefficients of the terms θ, $\sin\theta$, $\cos\theta$, $\theta\sin\theta$ and $\theta\cos\theta$, respectively, in each of the last three equations, one obtains 18 equations. Finally, solving the last 18 equations for A_i and C_i in terms of B_i ($i = 1-6$), one has

$$\begin{cases} A_1 = C^* B_2, \\ A_2 = 0, \\ A_3 = -B_4 + B_5, \\ A_4 = B_3 + B_6, \\ A_5 = -B_6, \\ A_6 = B_5, \end{cases} \tag{23a}$$

$$\begin{cases} C_1 = B_1, \\ C_2 = B_2, \\ C_3 = -2B_6, \\ C_4 = 2B_5, \\ C_5 = 0, \\ C_6 = 0, \end{cases} \tag{23b}$$

where

$$C^* = 1/(1 + r_e^*), \tag{24}$$

$$r_e^* = EI_y/(R^2 EA), \tag{25}$$

Similar to Eq. (18), if one sets

$$B_1 = G_5, \quad B_i = G_{i-1} \quad (i = 2{-}5), \quad B_6 = G_6, \tag{26}$$

substituting Eq. (26) into Eq. (23) and inserting the resulting values of A_i, B_i and C_i ($i = 1{-}6$) into Eqs. 1(a)–(c) one arrives at

$$\begin{aligned} u_x = {} & G_1 C^* + G_2 \cos\theta - G_3 \sin\theta + G_4(\theta \cos\theta + \sin\theta) \\ & + G_6(-\theta \sin\theta + \cos\theta), \end{aligned} \tag{27a}$$

$$u_\theta = G_1\theta + G_2 \sin\theta + G_3 \cos\theta + G_4\theta \sin\theta + G_5 + G_6\theta \cos\theta, \tag{27b}$$

$$\psi_y = \frac{1}{R}[G_1\theta + G_4(2\cos\theta) + G_5 + G_6(-2\sin\theta)]. \tag{27c}$$

For the case of neglecting SD, one has

$$r_s = EI_y/k'GAR^2 = 0 \tag{28}$$

and from Eqs. (14)–(17), (24) and (25), one obtains

$$S_1 = 2, \quad S_2 = -1, \quad C^* = 1/(1 + r_e^*). \tag{29}$$

In such situation, the displacement functions defined by Eq. 19(a)–(c) for the Timoshenko arch element (with SD considered) are exactly identical to the corresponding ones defined by Eqs. (27a)–(27c) for the Euler arch element (with SD neglected). Therefore, introducing the parameter C^* appearing in Eq. (27a) to Eq. (19a) will give the following displacement functions available for both the Timoshenko arch element and the Euler arch element:

$$\begin{aligned} u_x = {} & G_1 C^* + G_2 \cos\theta - G_3 \sin\theta + G_4(\theta \cos\theta - S_2 \sin\theta) \\ & + G_6(-\theta \sin\theta - S_2 \cos\theta), \end{aligned} \tag{30a}$$

$$u_\theta = G_1\theta + G_2 \sin\theta + G_3 \cos\theta + G_4\theta \sin\theta + G_5 + G_6\theta \cos\theta, \tag{30b}$$

$$\psi_y = \frac{1}{R}[G_1\theta + G_4(S_1 \cos\theta) + G_5 + G_6(-S_1 \sin\theta)]. \tag{30c}$$

It is noted that the last equations are exactly identical to Eqs. (19a)–(19c) except that the constant term G_1 in Eq. (19a) is replaced by $G_1 C^*$ in Eq. (30a), where the parameter C^* was

defined by Eq. (24). It is also noted that there exists an important relationship among r_e, r_s and r_e^* as one may see from Eqs. (8), (9) and (25): $r_e r_e^* = r_s$.

3. Element stiffness matrix

To write Eq. (30) in matrix form gives

$$\{u\} = [H]\{G\}, \tag{31}$$

where

$$\{u\} = \{\, u_x \quad u_\theta \quad \psi_y \,\}, \tag{32a}$$

$$[H] = \begin{bmatrix} C^* & \cos\theta & -\sin\theta & \theta\cos\theta - S_2\sin\theta & 0 & -\theta\sin\theta - S_2\cos\theta \\ \theta & \sin\theta & \cos\theta & \theta\sin\theta & 1 & \theta\cos\theta \\ \theta/R & 0 & 0 & S_1\cos\theta/R & 1/R & -S_1\sin\theta/R \end{bmatrix}, \tag{32b}$$

$$\{G\} = \{\, G_1 \quad G_2 \quad G_3 \quad G_4 \quad G_5 \quad G_6 \,\}. \tag{32c}$$

Applying to Eq. (31) the boundary conditions at the two ends of the arch element shown in Fig. 1, one obtains

$$\{\delta\} = [B]\{G\}, \tag{33}$$

where

$$\{\delta\} = \{\, u_{x1} \quad u_{\theta 1} \quad \psi_{y1} \quad u_{x2} \quad u_{\theta 2} \quad \psi_{y2} \,\}, \tag{34a}$$

$$[B] = \left[\begin{array}{cccccc} C^* & \cos\theta_1 & -\sin\theta_1 & \theta_1\cos\theta_1 - S_2\sin\theta_1 & 0 & -\theta_1\sin\theta_1 - S_2\cos\theta_1 \\ \theta_1 & \sin\theta_1 & \cos\theta_1 & \theta_1\sin\theta_1 & 1 & \theta_1\cos\theta_1 \\ \theta_1/\mathrm{R} & 0 & 0 & \mathrm{S}_1\cos\theta_1/\mathrm{R} & 1/\mathrm{R} & -\mathrm{S}_1\sin\theta_1/\mathrm{R} \\ \hline C^* & \cos\theta_2 & -\sin\theta_2 & \theta_2\cos\theta_2 - S_2\sin\theta_2 & 0 & -\theta_2\sin\theta_2 - S_2\cos\theta_2 \\ \theta_2 & \sin\theta_2 & \cos\theta_2 & \theta_2\sin\theta_2 & 1 & \theta_2\cos\theta_2 \\ \theta_2/\mathrm{R} & 0 & 0 & \mathrm{S}_1\cos\theta_2/\mathrm{R} & 1/\mathrm{R} & -\mathrm{S}_1\sin\theta_2/\mathrm{R} \end{array}\right] \tag{34b}$$

From Eq. (33) one obtains the integration constants $G_1 - G_6$ to be given by

$$\{G\} = [B]^{-1}\{\delta\} \tag{35}$$

Substituting Eq. (19) into Eq. (2), for the case of considering the effect of SD, and Eq. (27) into Eq. (20), for the case of neglecting the effect of SD, using the following relationship for the equilibrium of nodal forces:

$$\{\, F_{x1} \quad F_{\theta 1} \quad M_{y1} \,\} = -\{\, F_{x2} \quad F_{\theta 2} \quad M_{y2} \,\} \tag{36}$$

and then combining the results, one obtains

$$\{F\} = [D]\{G\}, \tag{37}$$

where

$$\{F\} = \{\, F_{x1} \quad F_{\theta 1} \quad M_{y1} \quad F_{x2} \quad F_{\theta 2} \quad M_{y2} \,\}, \tag{38}$$

$$[D]=\frac{EI_y}{R^2}\left[\begin{array}{ccc:ccc} 0 & 0 & 0 & -S_1\cos\theta_1/R & 0 & S_1\sin\theta_1/R \\ 0 & 0 & 0 & -S_1\sin\theta_1/R & 0 & -S_1\cos\theta_1/R \\ -C^* & 0 & 0 & S_1\sin\theta_1 & 0 & S_1\cos\theta_1 \\ \hdashline 0 & 0 & 0 & S_1\cos\theta_2/R & 0 & -S_1\sin\theta_2/R \\ 0 & 0 & 0 & S_1\sin\theta_2/R & 0 & S_1\cos\theta_2/R \\ C^* & 0 & 0 & -S_1\sin\theta_2 & 0 & -S_1\cos\theta_2 \end{array}\right] \tag{39}$$

Substituting the values of $\{G\}$ defined by Eq. (35) into Eq. (37), one obtains

$$\{F\} = [D][\mathrm{B}]^{-1}\{\delta\} = [K]\{\delta\}, \tag{40}$$

where $[K]$ is the stiffness matrix for the arch element given by

$$[K] = [D][B]^{-1}. \tag{41}$$

The stiffness matrix obtained from Eq. (41) with $C^* = 1$ is for the arch element by considering the effect of SD, while with $C^* = 1/(1 + r_e^*)$, $r_e^* = EI_y/(R^2EA)$ and $r_s = RI_y/(k'GAR^2) = 0$ is for the arch element by neglecting the effect of SD.

4. Element mass matrix

The kinetic energy of an arch element is given by [9]

$$T = \frac{1}{2}\int_{\theta_1}^{\theta_2}[\rho A(\dot{u}_x^2 + \dot{u}_\theta^2) + \rho I_y\dot{\psi}_y^2]R\,\mathrm{d}\theta, \tag{42}$$

where the dots denote the derivatives with respect to time t, ρ is the mass density of the arch material and I_y is the moment of inertia of the cross-sectional area defined by Eq. (3). The third term on the right-hand side of Eq. (42), $\rho I_y\dot{\psi}_y^2$, represents the RI, which is not considered in Refs. [1,9]. Since, the effect of SD has been included in the displacement functions, u_x, u_θ and ψ_y, so does in the kinetic energy given by Eq. (42).

For harmonic free vibrations, one has

$$\{u\} = \{\bar{u}\}\mathrm{e}^{\mathrm{i}\omega t}, \tag{43}$$

where $\{\bar{u}\}$ is the amplitude of $\{u\}$, ω is the natural frequency of the arch, t is time and $\mathrm{i} = \sqrt{-1}$.

The substitution of Eqs. (30) and (43) into Eq. (42) yields

$$T = \tfrac{1}{2}\omega^2\{\delta\}^{\mathrm{T}}[M]\{\delta\}, \tag{44}$$

where $[M]$ is the consistent mass matrix for an arch element given by

$$[M] = \rho R([B]^{-1})^{\mathrm{T}}\left(\int_{\theta_1}^{\theta_2}[H]^{\mathrm{T}}[\Lambda][H]\,\mathrm{d}\theta\right)[B]^{-1} \tag{45}$$

with

$$[\Lambda] = \begin{bmatrix} A & 0 & 0 \\ 0 & A & 0 \\ 0 & 0 & I_y \end{bmatrix}. \tag{46}$$

To determine the consistent mass matrix of an arch element $[M]$, using Eq. (45), it is required to calculate the following integration:

$$[\bar{H}] = \int_{\theta_1}^{\theta_2} [H]^{\mathrm{T}}[\Lambda][H]\,\mathrm{d}\theta \tag{47}$$

and all the other numerical calculations are performed by computer. The results for the integration defined by Eq. (47) are shown in Appendix A at the end of this paper. Because $[\bar{H}]$ is a 6×6 symmetrical square matrix, one requires only to calculate the 21 coefficients of the matrix. This will be much simpler than the 108 constants for the 18 shape functions shown in Tables 1–3 of Ref. [8]. It is noted that the mass matrix for the arch element considering the effect of SD should be obtained from Eq. (45) with $C^* = 1$, while that for the arch element neglecting the effect of SD should be obtained from Eq. (45) with $C^* = 1/(1 + r_e^*)$, $r_e^* = EI_y/(R^2EA)$ and $r_s = RI_y/(k'GAR^2) = 0$.

For the purpose of comparison, the free vibration analysis was also performed using the following lumped mass matrix for the arch element:

$$[M^*] = \ulcorner m_1 \quad m_1 \quad J_1 \quad m_2 \quad m_2 \quad J_2 \urcorner \tag{48}$$

with

$$m_1 = m_2 = \tfrac{1}{2}\rho AR\alpha, \tag{49a}$$

$$J_1 = J_2 = \tfrac{1}{2}\rho I_y R\alpha. \tag{49b}$$

The symbol $\ulcorner \cdot \urcorner$ in Eq. (48) denotes a diagonal matrix and the notation α $(= \theta_2 - \theta_1)$ in Eq. (49) denotes the subtended angle of the arch element (see Fig. 1).

5. Numerical results and discussions

This section validates the accuracy of the presented approach and studies the effec of SD and that of RI. The influence of thickness ratio (a/R) on the natural frequencies and mode shapes of the Euler arch, the rotary arch and the Timoshenko arch are also investigated, where the Euler arch refers to an arch with the effects of both SD and RI neglected, the rotary arch refers to an arch with only the effect of RI considered, while the Timoshenko arch refers to an arch with the effects of both SD and RI considered. In the finite element method (FEM), the element stiffness matrix and mass matrix for an Euler arch, a rotary arch or a Timoshenko arch take the same forms, the only difference between them is the values for the coefficients of the element property matrices. For the Euler arch element one must set the terms regarding SD and RI to be equal to zero in the associated coefficients for the element property matrices, while for the rotary arch one only requires setting the terms regarding SD to be equal to zero. It is also noted in the FEM that, either for the Euler arch or the rotary arch, the ''rotational'' degree of freedom (d.o.f.), such as ψ_y in Fig. 1, must also be considered in addition to the ''translational'' d.o.f. This is different from the classical analytical method, where the translational (lateral) displacement is the only independent variable for an Euler arch.

5.1. Validation of natural frequencies

The given data for the first example are (cf. Fig. 2): average radius $R = 30''$, total subtended angle $\bar{\alpha} = 1.0\,\text{rad} = 57.3^\circ$, radial thickness $a = 0.01289''$, axial thickness $b = 1.008''$, cross-sectional area $A = ab = 0.013\,\text{in}^2$, mass density of arch material $\rho = 0.1\,\text{lb/in}^3$ and Young's modulus $E = 10^7\,\text{lb/in}^2$. If the two ends of the arch are simply supported (i.e., $u_{x1} = u_{xn} = 0$ with n being the numbering of the final node), then the lowest five natural frequencies of the Euler arch are shown in Table 1, where the exact solutions listed in Column 2 are determined by using the frequency equation given in Appendix A of Ref. [9]. Columns 3–5 of Table 1 show the lowest five natural frequencies of the simply supported arch obtained from the presented approach using 2, 4 and 6 arch elements, respectively. Comparing the last natural frequencies with the exact solutions listed in Column 2 of Table 1, one sees that the presented approach with 6 arch elements (i.e., $N_e = 6$) will achieve excellent accuracy for the lowest five natural frequencies.

If the given data for the arch were changed to the ones given by Ref. [11]: $R = 1\,\text{m}$, $\bar{\alpha} = 2\pi/3\,\text{rad}$, $\rho = 1\,\text{kg/m}^3$, $E = 1\,\text{N/m}^2$, the dimensions of the cross-section being $a = b = 0.25$–$0.01\,\text{m}$, and the Poisson ratio $v = 0.3$, shear modulus $G = E/[2(1+v)] = 0.384\,\text{N/m}^2$, shear coefficient $k' = 0.833$, then the lowest three natural frequencies for the "clamped–clamped"

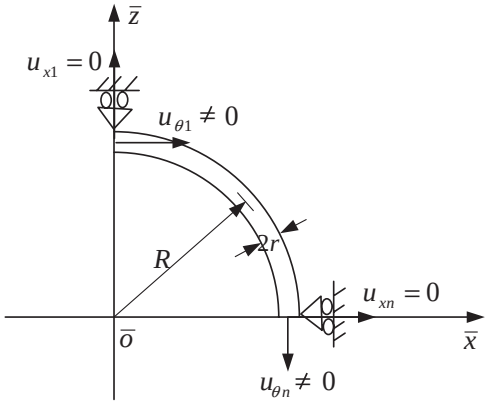

Fig. 2. Natural frequencies of a free–free complete ring may be determined by using a simply supported quarter ring.

Table 1
Lowest five natural frequencies of the simply supported curved beam, ω_i ($i = 1$–5) (rad/s), with the effects of both SD and RI neglected

Mode no. i	Exact solutions [9]	Total number of arch elements, N_e		
		2	4	6
1	0.349	0.349	0.349	0.349
2	1.571	1.572	1.572	1.572
3	3.612	3.725	3.615	3.613
4	6.470	8.212	6.474	6.474
5	10.144	14.307	10.274	10.162

Table 2
(a) Lowest three natural frequencies for the clamped–clamped *Timoshenko* arch and (b) lowest three natural-frequency ratios, $\omega_i^{0e}/\omega_i^{de}$, for the clamped–clamped *rotary* arch obtained from Ref. [11] and present paper

Thickness ratios, a/R	Methods	Natural frequencies (rad/s)[a]		
		ω_1^{de}	ω_2^{de}	ω_3^{de}
(a)				
0.250	Ref. [11]	0.6878	0.8219	1.4877
	Present	0.6898	0.8225	1.4910
0.100	Ref. [11]	0.3282	0.5876	0.9810
	Present	0.3284	0.5878	0.9811
0.050	Ref. [11]	0.1692	0.3295	0.6022
	Present	0.1692	0.3295	0.6022
0.025	Ref. [11]	0.08528	0.1690	0.3076
	Present	0.08528	0.1690	0.3076
0.010	Ref. [11]	0.03419	0.06808	0.1238
	Present	0.03419	0.06808	0.1238
(b)		Natural-frequency ratios, $\omega_i^{0e}/\omega_i^{de}$[b]		
		$\omega_1^{0e}/\omega_1^{de}$	$\omega_2^{0e}/\omega_2^{de}$	$\omega_3^{0e}/\omega_3^{de}$
0.250	Ref. [11]	1.1716	1.0291	1.1397
	Present	1.1845	1.0360	1.1508
0.100	Ref. [11]	1.0329	1.0417	1.0130
	Present	1.0357	1.0477	1.0257
0.050	Ref. [11]	1.0089	1.0143	1.0208
	Present	1.0098	1.0189	1.0344
0.025	Ref. [11]	1.0021	1.0036	1.0055
	Present	1.0029	1.0073	1.0162
0.010	Ref. [11]	1.0003	1.0006	1.0008
	Present	1.0005	1.0020	1.0056

[a] ω_i^{de} is the ith natural frequency with all effects (including axial compressibility, rotary inertia and shear deformation) considered as given by Table 6 of Ref. [11].
[b] ω_i^{0e} is the ith natural frequency with shear deformation neglected as given by Table 6 of Ref. [11].

Timoshenko arch are shown in Table 2(a) and those for *rotary* arch are shown in Table 2(b) corresponding to the five thickness ratios, $a/R = 0.250$, 0.100, 0.050, 0.025, 0.010. Here ω_i^{de} represents the ith natural frequency with all effects (including axial compressibility, RI and SD) considered as given by Table IV of Ref. [11], and ω_i^{0e} denotes the ith natural frequency with SD

Table 3
(a) Lowest several natural-frequency parameters of the free–free ring, $\beta_i = \omega_i\sqrt{\rho AR^4/(EI_y)}$, $i = 2$–4 and (b) lowest natural-frequency parameters of the circular arcs with hinged–hinged and fixed–fixed supporting conditions, $\beta_1 = \omega_1\sqrt{\rho AR^4/(EI_y)}$
(a)

Mode no. i	Euler ring		Rotary ring		Timoshenko ring	
	Table 1 of [15]	Present	Table 1 of [15]	Present	Table 1 of [15]	Present
2	2.680	2.682	2.671	2.676	2.631	2.624
3	7.600	—	7.530	—	7.292	—
4	14.550	14.539	14.310	14.306	13.570	13.539

(b)

Subtended angles $\bar{\alpha}$ (deg)	Supporting conditions	Euler arch		
		Table 2 of [15]	Den Hartog [16]	Present
80	Hinged–hinged	17.610	17.800	17.764
180		2.105	2.200	2.260
240		0.721	0.796	0.817
360		0.000	0.000	0.000
100	Fixed–fixed	17.850	17.900	17.543
270		1.245	1.395	1.390
320		0.813	0.821	0.819
360		0.547	0.567	0.565

neglected as given by Table VI of Ref. [11]. In other words, ω_i^{de} and ω_i^{0e} represent the ith natural frequency of the *Timoshenko* arch and the *rotary* arch, respectively. From Tables 2(a) and 2(b) one sees that the numerical results of the present paper are very close to those of Ref. [11] in the range of thickness ratios, $a/R = 0.250$ (for thick arch) to 0.010 (for thin arch). The total number of arch elements for this example is $N_e = 32$.

Finally, the lowest several natural-frequency parameters, $\beta_i = \omega_i\sqrt{\rho AR^4/(EI_y)}$, $i = 1, 2, \ldots$, for the complete circular ring and the circular arcs of Refs. [15,16] were studied. The given data are [15,16]: $I_y/AR^2 = 0.0025$, $E/k'G = 3.0$, $I_y = \pi r^4/4$ and $r/R = 0.1$, where k' is the shear coefficient, G is the shear modulus and r is the radius for the circular cross-section of the arch. To achieve the values of the last non-dimensional parameters, in this paper, the following material constants and arch dimensions were used: $k' = 0.8$, $\nu = 0.2$, $E = 30 \times 10^6\,\mathrm{N/m^2}$, $\rho = 7.329 \times 10^{-4}\,\mathrm{kg/m^3}$, $r = 1\,\mathrm{m}$ and $R = 10\,\mathrm{m}$. In addition, the simply supported quarter ring shown in Fig. 2 was used to determine the natural frequencies of the free–free complete ring. Table 3(a) shows the values of β_i ($i = 2, 3, 4$) for the free–free complete ring, while Table 3(b) shows the fundamental (lowest) frequency parameters (β_1) for the hinged–hinged circular arcs with subtended angles $\bar{\alpha} = 80^\circ$, 180°, 240°, 360° and those for the fixed–fixed circular arcs with subtended angles $\bar{\alpha} = 100^\circ$, 270°, 320°, 360°. It is evident that all the numerical results of the present paper are in good agreement with those of Refs. [15,16]. The total number of arch elements for this example is $N_e = 10$. Since, for a free–free ring, the first mode (i.e., $i = 1$) is a rigid-body mode with zero natural frequency, it is not shown in Table 3(a). Besides, a hinged–hinged circular arc with total

subtended angle $\bar{\alpha}=360^\circ$ is equivalent to a complete ring supported by a pin. Thus, its first mode is also a rigid-body mode with zero natural frequency as shown in the 6th row of Table 3(b).

5.2. Influence of SD and RI on "Thin" arch

The arch studied in this subsection is a 180° in-plane circular curved beam shown in Fig. 3 with the following given data: $a=0.06\,\mathrm{m}$, $b=0.04\,\mathrm{m}$, $R=0.5\,\mathrm{m}$, $A=ab=0.0024\,\mathrm{m}^2$, $E=12\times10^{10}\,\mathrm{N/m}^2$, $\rho=7.2\times10^3\,\mathrm{kg/m}^3$, $\nu=0.2$, $k'=0.833$, $G=E/[2(1+\nu)]=5\times10^{10}\,\mathrm{N/m}^2$ and the total number of arch elements was $N_e=20$. Table 4 shows the influence of SD and RI on the lowest five natural frequencies of the arch with three supporting conditions: (a) clamped–clamped (C–C), (b) clamped—hinged (C–H) and (c) hinged–hinged (H–H). From Table 4(a) one sees that the lowest five natural frequencies of the Euler arch (see Columns 2 and 3) are very close to those of the rotary arch (see Columns 4 and 5). Thus, the effect of RI on the current thin arch with thickness ratio $a/R=0.06/0.5=0.12$ is very small. The differences between the lowest five natural frequencies of the Timoshenko arch (see Columns 6 and 7 of Table 4(a)) and those of the rotary or Euler arch are larger, but they are still not significant (about 2.2% for the fundamental frequencies), thus, the effect of SD on the current thin arch (with $a/R=0.12$) is also small.

In Table 4(a), the natural frequencies listed in Columns 2, 4 and 6 were obtained from the consistent-mass model and those in Columns 3, 5 and 7 were obtained from the lumped-mass model. It is evident that, for the Euler arch, rotary arch and the Timoshenko arches, the lowest five natural frequencies obtained from the consistent-mass model are very close to the corresponding ones obtained from the lumped-mass model. This is the reason why the lowest five mode shapes of the C–C Timoshenko arch obtained from the consistent-mass model are also very close to the corresponding ones obtained from the lumped-mass model as shown in Fig. 4, where the long dashed line (— — —) represents the static (un-deformed) configuration of the C–C Timoshenko arch, while the short dash lines (- - - - - - - - - - -) and the solid lines (———) denote the mode shapes obtained from the lumped-mass model and the consistent-mass model, respectively. It is noted that the ordinate of Fig. 4 and the ones of Figs. 5–7 denote the ith modal displacements in the vertical ($\bar{z}$) direction determined by (cf. Fig. 1)

$$\{\tilde{u}_{\bar{z}}^*\}_i=-\cos[\theta]\{\tilde{u}_{\bar{x}}^*\}_i+\sin[\theta]\{\tilde{u}_{\theta}^*\}_i, \tag{50}$$

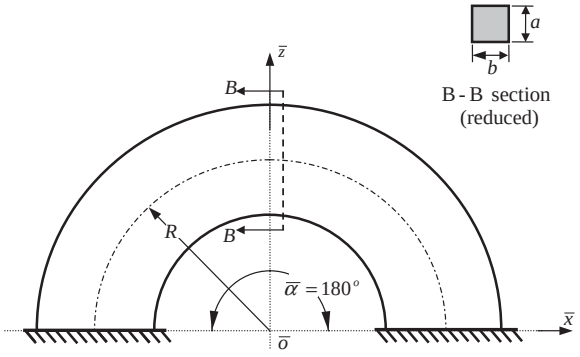

Fig. 3. Nomenclature for a 180° circular arch.

Table 4
Influence of SD and RI on the lowest five natural frequencies of a "thin" arch with three supporting conditions: (a) clamped–clamped; (b) clamped–hinged; and (c) hinged–hinged

Mode no. i	Euler arch		Rotary arch		Timoshenko arch	
	Consistent-mass model	Lumped-mass model	Consistent-mass model	Lumped-mass model	Consistent-mass model	Lumped-mass model
(a)						
1	1236.435	1236.400	1234.953	1234.918	1209.620	1209.485
2	2672.403	2672.124	2663.102	2662.838	2574.673	2573.079
3	4988.269	4986.379	4950.186	4948.450	4721.978	4712.167
4	6756.161	6752.289	6716.738	6713.089	6492.510	6465.832
5	8884.755	8876.469	8799.000	8791.400	8551.011	8490.021
(b)						
1	918.726	918.711	917.723	917.708	904.519	904.464
2	2306.551	2306.374	2298.939	2298.769	2240.723	2239.690
3	4443.122	4441.864	4410.243	4409.068	4248.178	4241.003
4	6560.629	6557.043	6509.646	6506.297	6268.102	6244.088
5	8395.823	8389.178	8335.402	8329.079	8225.623	8171.793
(c)						
1	641.003	640.998	640.402	640.397	634.499	634.479
2	1947.919	1947.814	1941.907	1941.804	1907.409	1906.746
3	3933.185	3932.360	3905.235	3904.450	3796.761	3791.435
4	6223.602	6220.599	6163.089	6160.286	5942.490	5921.688
5	8150.610	8144.730	8115.855	8110.1143	8098.707	8047.228

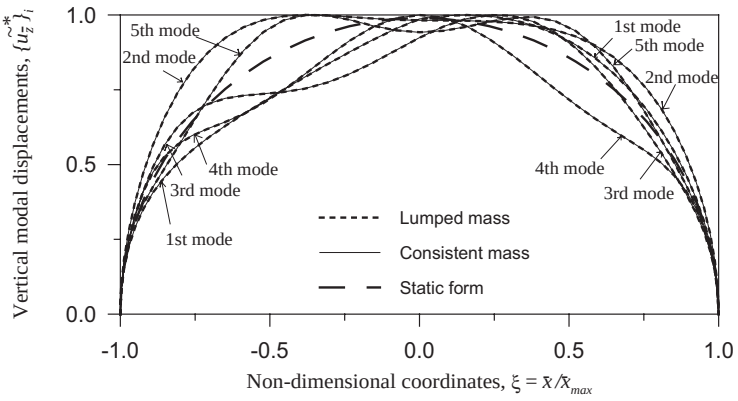

Fig. 4. Lowest five mode shapes of the 180° C–C circular thin Timoshenko arch obtained from the consistent-mass model (——) and the lumped-mass model (------).

where $\{\tilde{u}_x^*\}_i$ and $\{\tilde{u}_\theta^*\}_i$ are the modal displacements in the radial and circumferential directions, respectively, and $[\theta]$ is a diagonal matrix with its diagonal coefficients composed of the angular co-ordinates for all nodal points of the entire arch.

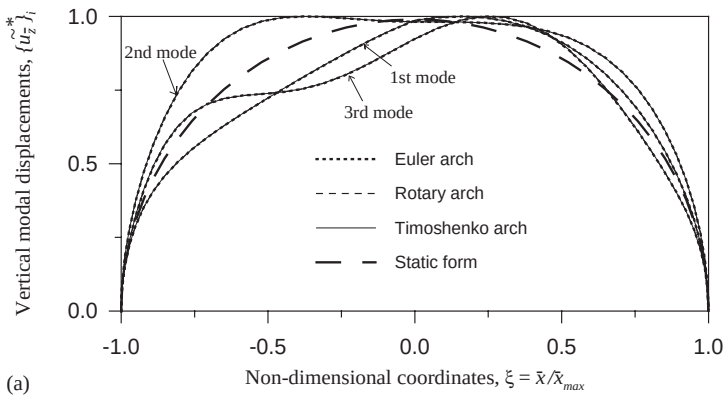

(a)

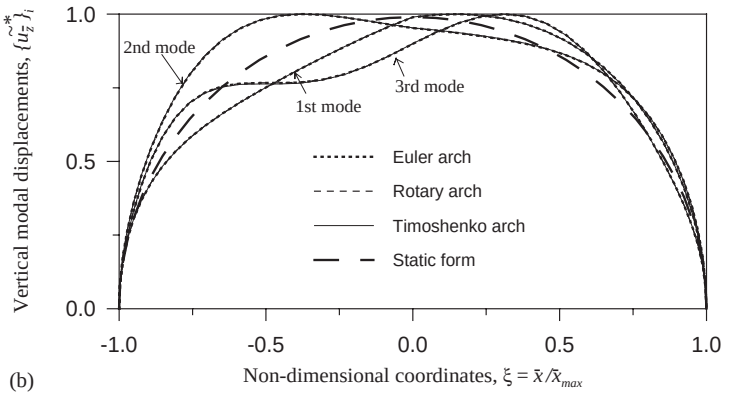

(b)

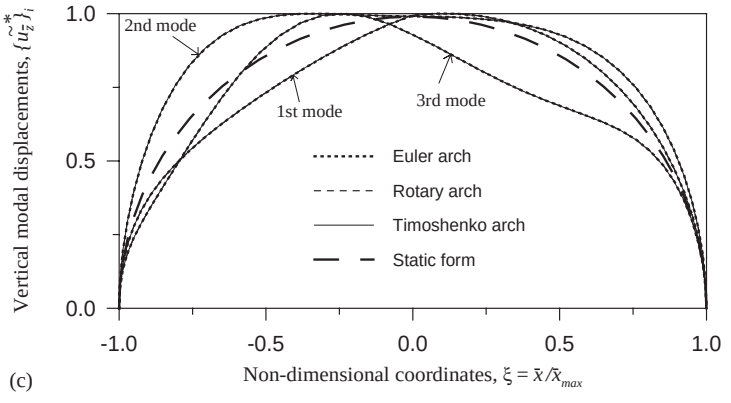

(c)

Fig. 5. Lowest three mode shapes of the 180° thin Euler arch (……), shear arch (------) and Timoshenko arch (———) obtained from the consistent-mass model with three supporting conditions: (a) C–C; (b) C–H; and (c) H–H.

The lowest five natural frequencies of the 180° arch with C–H and H–H supporting conditions are shown in Tables 4(b) and (c), respectively. Comparing Tables 4(b) and (c) with Table 4(a), one sees that all conclusions for the lowest five natural frequencies of Euler arch, rotary arch and

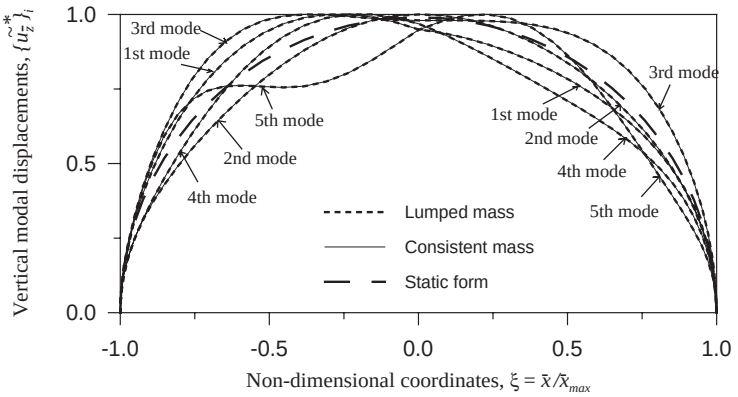

Fig. 6. Lowest five mode shapes of the 180° C–C circular thick Timoshenko arch obtained from the consistent-mass model (——) and the lumped-mass model (------).

Timoshenko arches obtained from Table 4(a) in the last paragraphs are also valid for those shown in Tables 4(b) and (c). Since the lowest three natural frequencies of the Euler arch are very close to those of the rotary arch and those of the Timoshenko arch, so are the corresponding mode shapes as one may see from Fig. 5(a) for the C–C arch, from Fig. 5(b) for the C–H arch and from Fig. 5(c) for the H–H arch. It is similar to Fig. 4 that the long dashed lines (— — —) represent the static (un-deformed) configurations of the arches in Figs. 5(a–c), while the dotted lines (……), the short dashed lines (--------) and the solid lines (———) denote the mode shapes for Euler arches, rotary arches and Timoshenko arches, respectively. To avoid confusion, only the lowest three mode shapes were shown in Fig. 5.

5.3. *Influence of SD and RI on "Thick" arch*

All the given data for the arch studied in this subsection are exactly the same as those studied in the last subsection. The only difference is that the thickness ratio of the current arch is much larger than that of the arch studied in the last subsection. In other words, for convenience, the arch studied in the last subsection is called the thin arch (with $a/R = 0.06/0.5 = 0.12$) and that studied in this subsection is called the thick arch. The dimensions for the cross-section of the current arch are: $a = 0.25\,\text{m}$, $b = 0.25\,\text{m}$ and $A = ab = 0.0625\,\text{m}^2$. Thus, its thickness ratio is $a/R = 0.25/0.5 = 0.5$.

It is similar to Table 4 that Table 5 shows the lowest five natural frequencies of Euler arch, rotary arch and Timoshenko arch with three supporting conditions: (a) C–C, (b) C–H and (c) H–H obtained from the consistent-mass model and the lumped-mass model. Although the lowest five natural frequencies obtained from the consistent-mass model are also very close to those obtained from the lumped-mass model, the lowest five natural five natural frequencies of the Euler arch or the rotary arch are much greater than the corresponding ones of the Timoshenko arch. This is the reason why the lowest five mode shapes obtained from the consistent-mass model are also very close to those obtained from the lumped-mass model as shown in Fig. 6, but the lowest three mode shapes of the Euler arch or the rotary arch are different from the corresponding ones of the Timoshenko arch as one may see from Fig. 7(a) for the C–C arches, Fig. 7(b) for the

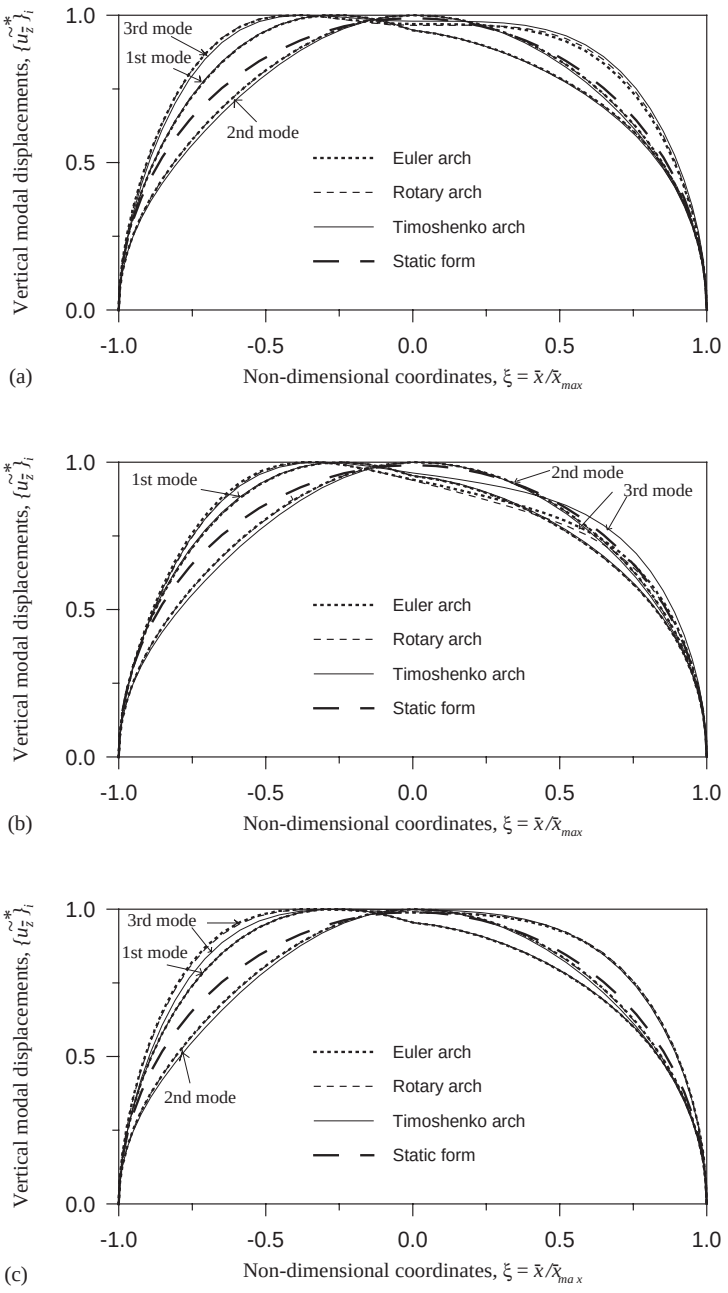

Fig. 7. Lowest three mode shapes of the 180° thick Euler arch (……), shear arch (------) and Timoshenko arch (———) obtained from the consistent-mass model with supporting conditions: (a) C–C; (b) C–H; and (c) H–H.

C–H arches and Fig. 7(c) for the H–H arches. It is seen that the divergence between the corresponding mode shapes increases with the increase of mode number i. It is similar to Fig. 5 that, to avoid confusion, only the lowest three mode shapes were shown in Fig. 7.

Table 5
Influence of SD and RI on the lowest five natural frequencies of a "thick" arch with three supporting conditions: (a) clamped–clamped; (b) clamped–hinged; and (c) hinged–hinged

Mode no. i	Euler arch		Rotary arch		Timoshenko arch	
	Consistent-mass model	Lumped-mass model	Consistent-mass model	Lumped-mass model	Consistent-mass model	Lumped-mass model
(a)						
1	4835.399	4833.356	4762.023	4760.131	3745.324	3742.190
2	6505.408	6504.149	6444.462	6443.319	5795.380	5780.251
3	10756.212	10737.192	10403.312	10384.522	9764.621	9687.206
4	13196.301	13179.992	12462.042	12451.134	9769.648	9715.820
5	18215.823	18084.990	17477.952	17341.736	14113.887	13897.792
(b)						
1	3690.404	3689.597	3631.343	3630.606	3010.172	3008.534
2	6495.035	6493.733	6429.795	6428.622	5728.944	5714.474
3	10570.244	10551.029	10232.081	10213.305	9122.353	9059.526
4	11412.132	11403.628	10790.988	10783.647	9769.431	9714.219
5	18111.764	17974.655	17430.608	17295.973	13551.757	13365.898
(c)						
1	2658.848	2658.562	2618.689	2618.431	2293.020	2292.297
2	6460.329	6458.944	6379.862	6378.666	5597.677	5584.355
3	9690.012	9686.462	9201.280	9197.816	8589.243	8536.110
4	10640.727	10620.073	10325.827	10305.154	9692.360	9636.890
5	17429.417	17398.258	15571.109	15547.527	13010.867	12852.972

6. Conclusions

1. A technique for deriving the displacement functions of an arch element has been presented in this paper. Comparing with the existing approaches, the presented technique has the advantages of being simple, straightforward and systematic. The formulation of this paper is available for both the thin arches (with SD negligible) and the thick arches (with SD significant).
2. If an arch with the effects of both SD and RI neglected is called the Euler arch, that with only the effect of RI considered is called the rotary arch and that with the effects of both SD and RI considered is called the Timoshenko arch, then no matter whether the arch is an Euler arch (or thin arch), a rotary arch or a Timoshenko arch (or thick arch), its lowest five natural frequencies and the associated mode shapes obtained from the simple lumped-mass model are very close to the corresponding ones obtained from the complicated consistent-mass model. Thus, it is one of the simple ways for checking the availability of a new approach by using the simple lumped-mass model.
3. The effect of SD on the lowest five natural frequencies is negligible for the thin arch and significant for the thick arch, this is also true for the associated mode shapes, particularly for the higher modes.

4. Among the SD and the RI, the effect on the dynamic behavior of an arch of the SD is much greater than that of the RI.

Acknowledgements

This paper is part of the extension of the project under NSC89-2611-E-006-049, National Science Council, Republic of China.

Appendix A. Coefficients of matrix $[\bar{H}]$

Integration according to Eq. (47) will give the coefficients of the matrix $[\bar{H}]$, $\bar{H}_{ij}$ $(i,j = 1-6)$. Because of symmetry, only the coefficients in the left lower triangle are shown below:

$$\bar{H}_{11} = \left[A(C^*)^2\theta + \left(A + \frac{I_y}{R^2}\right)\left(\frac{\theta^3}{3}\right)\right]_{\theta_1}^{\theta_2},$$

$$\bar{H}_{21} = A[(1 + C^*)\sin\theta - \theta\cos\theta]_{\theta_1}^{\theta_2},$$

$$\bar{H}_{22} = A[\theta]_{\theta_1}^{\theta_2},$$

$$\bar{H}_{31} = A[(1 + C^*)\cos\theta + \theta\sin\theta]_{\theta_1}^{\theta_2},$$

$$\bar{H}_{32} = 0,$$

$$\bar{H}_{33} = A[\theta]_{\theta_1}^{\theta_2},$$

$$\bar{H}_{41} = \left[\left(2A + AC^*(1 + S_2) + \frac{S_1 I_y}{R^2}\right)\cos\theta + \left(AC^* + 2A + \frac{S_1 I_y}{R^2}\right)\theta\sin\theta - A\theta^2\cos\theta\right]_{\theta_1}^{\theta_2},$$

$$\bar{H}_{42} = \frac{A}{2}[\theta^2 + S_2\cos^2\theta]_{\theta_1}^{\theta_2},$$

$$\bar{H}_{43} = \frac{AS_2}{2}[\theta - \sin\theta\cos\theta]_{\theta_1}^{\theta_2},$$

$$\bar{H}_{44} = \left[\frac{A\theta^3}{3} + \left(AS_2(1 + S_2) + \frac{S_1^2 I_y}{R^2}\right)\frac{\theta}{2} - \left(AS_2(1 + S_2) - \frac{S_1^2 I_y}{R^2}\right)\frac{\sin\theta\cos\theta}{2} - AS_2\theta\sin^2\theta\right]_{\theta_1}^{\theta_2},$$

$$\bar{H}_{51} = \left[\left(\frac{1}{2}\right)\left(A + \frac{I_y}{R^2}\right)\theta^2\right]_{\theta_1}^{\theta_2},$$

$$\bar{H}_{52} = A[-\cos\theta]_{\theta_1}^{\theta_2},$$

$$\bar{H}_{53} = A[\sin\theta]_{\theta_1}^{\theta_2},$$

$$\bar{H}_{54} = \left[\left(A + \frac{S_1 I_y}{R^2}\right)\sin\theta - A\theta\cos\theta\right]_{\theta_1}^{\theta_2},$$

$$\bar{H}_{55} = \left[\left(A + \frac{I_y}{R^2}\right)\theta\right]_{\theta_1}^{\theta_2},$$

$$\bar{H}_{61} = \left[-\left(AC^*(1+S_2) + 2A + \frac{S_1 I_y}{R^2}\right)\sin\theta + A\theta^2\sin\theta + \left(AC^* + 2A + \frac{S_1 I_y}{R^2}\right)\theta\cos\theta\right]_{\theta_1}^{\theta_2},$$

$$\bar{H}_{62} = \frac{-AS_2}{2}[\theta + \sin\theta\cos\theta]_{\theta_1}^{\theta_2},$$

$$\bar{H}_{63} = \frac{A}{2}[\theta^2 + S_2\sin^2\theta]_{\theta_1}^{\theta_2},$$

$$\bar{H}_{64} = \frac{1}{2}\left[-AS_2\left(\theta\sin 2\theta + \frac{\cos 2\theta}{2}\right) + \left(AS_2^2 - \frac{S_1^2 I_y}{R^2}\right)\sin^2\theta\right]_{\theta_1}^{\theta_2},$$

$$\bar{H}_{65} = \left[\left(A + \frac{S_1 I_y}{R^2}\right)\cos\theta + A\theta\sin\theta\right]_{\theta_1}^{\theta_2},$$

$$\bar{H}_{66} = \left[\frac{A\theta^3}{3} + \left(-AS_2(1-S_2) + \frac{S_1^2 I_y}{R^2}\right)\frac{\theta}{2} + \left(AS_2(1+S_2) - \frac{S_1^2 I_y}{R^2}\right)\frac{\sin\theta\cos\theta}{2} + AS_2\theta\sin^2\theta\right]_{\theta_1}^{\theta_2},$$

where

$$[f(\theta)]_{\theta_1}^{\theta_2} = f(\theta_2) - f(\theta_1).$$

References

[1] A.B. Sabir, D.G. Ashwell, A comparison of curved beam finite elements when used in vibration problems, *Journal of Sound and Vibration* 18 (4) (1971) 555–563.

[2] D.G. Ashwell, A.B. Sabir, T.M. Roberts, Further studies in the application of curved finite elements to circular arches, *International Journal of Mechanical Science* 13 (1971) 507–517.

[3] A.O. Lebeck, J.S. Knowlton, A finite element for the three-dimensional deformation of a circular ring, *International Journal for Numerical Methods in Engineering* 21 (1985) 421–435.

[4] R. Palaninathan, P.S. Chandrasekharan, Curved beam element stiffness matrix formulation, *Computers and Structures* 21 (4) (1985) 663–669.

[5] H.K. Stolarski, Y.M. Chiang, The mode-decomposition, C^0 formulation of curved, two-dimensional structural elements, *International Journal for Numerical Methods in Engineering* 28 (1989) 145–154.

[6] H.S. Ryu, H.C. Sin, Curved beam elements based on strained fields, *Communications in Numerical Methods in Engineering* 12 (1996) 767–773.
[7] P. Litewka, J. Rakowski, An efficient curved beam finite element, *International Journal for Numerical Methods in Engineering* 40 (1997) 2629–2652.
[8] P. Litewka, J. Rakowski, The exact thick arch finite element, *Computers and Structures* 68 (1998) 369–379.
[9] M. Petyt, C.C. Fleischer, Free vibration of a curved beam, *Journal of Sound and Vibration* 18 (1) (1971) 17–30.
[10] C.H. Yoo, J.P. Fehrenbach, Natural frequencies of curved girders, *Journal of the Engineering Mechanics Division, American Society of Civil Engineers* 107 (EM2) (1981) 339–354.
[11] P. Litewka, J. Rakowski, Free vibrations of shear-flexible and compressible arches by FEM, *International Journal for Numerical Methods in Engineering* 52 (2001) 273–286.
[12] S.K. Chaudhuri, S. Shore, Dynamic analysis of horizontally curved I-girder bridges, *Journal of the Structural Division, American Society of Civil Engineers* 103 (ST8) (1977) 1589–1604 (Proc. Paper 13121, August).
[13] S.K. Chaudhuri, S. Shore, Thin walled curved beam finite element, *Journal of the Engineering Mechanics Division, American Society of Civil Engineers* 103 (1977) 921–937.
[14] J.S. Wu, L.K. Chiang, Free vibration analysis of arches using curved beam elements, *International Journal for Numerical Methods in Engineering* 58 (13) (2003) 1907–1936.
[15] S.S. Rao, V. Sundararajan, In-plane flexural vibration of circular rings, *Journal of Applied Mechanics, American Society Mechanical Engineers* 36 (1969) 620–625.
[16] J.P. Den Hartog, Vibration of frames of electrical machines, *Journal of Applied Mechanics*, American Society of Mechanical Engineers 50 (1928) APM-50-6.